Measurement of Cu(II) Copper Defect Dipoles in Ferroelectric $PbTiO_3$ Using Electron-Nuclear Double Resonance

R. R. Garipov,[1] J.-M. Spaeth,[2] and D. J. Keeble[1,*]

[1]*Carnegie Laboratory of Physics, School of Engineering, Physics, and Mathematics, University of Dundee, Dundee DD1 4HN, United Kingdom*

[2]*Fakultät Naturwissenschaften, Department Physik, Universität Paderborn, D-33095 Paderborn, Germany*

(Received 19 September 2008; published 12 December 2008)

Point defects associated with Cu(II) in ferroelectric $PbTiO_3$ were determined using pulsed electron-nuclear double resonance (ENDOR). Three centers were observed, and neighbor ^{207}Pb superhyperfine tensors to the third shell of equivalent Pb ions measured. The ENDOR angular dependence showed that Cu(II) is incorporated as an acceptor at the Ti site. One center also showed ENDOR from an axial fluorine ion. The three defects were determined to be the Cu(II)–oxygen-vacancy defect dipole, Cu(II) with a complete oxygen octahedron, and a Cu(II)-F^- defect dipole center.

DOI: 10.1103/PhysRevLett.101.247604 PACS numbers: 77.84.Dy, 61.72.Hh, 76.30.Fc

Lead titanate (Fig. 1) is a model ferroelectric perovskite oxide, ABO_3, with a transition from a high temperature cubic paraelectric phase to a tetragonal ferroelectric phase at 763 K. It is the end member of several technologically important solid solution phase fields, including $Pb(Zr_xTi_{1-x})O_3$ (PZT). These materials are used in applications ranging from ferroelectric random access memories to high strain actuators. Point defects are of special importance as, in addition to their conventional role as charge traps in these high band gap semiconductor materials ($E_g \sim 3.2$ eV), they can couple directly to ferroelectric polarization. Defect complexes with a net dipole moment are particularly effective and can impede polarization reversal. An important example of a defect dipole is an acceptor, an impurity with a negative local charge with respect to the site of substitution and a charge compensating positively charged defect, typically an oxygen vacancy, at a nearest neighbor position. Common acceptor impurities include Fe^{3+}, Al^{3+}, Cr^{3+}, and Cu^{2+}, which are assumed to substitute for Ti^{4+} at the B site (Fig. 1). Aligned defect dipoles generate an internal bias field, which strongly affects the ferroelectric behavior [1–5]. Mechanisms for aging and fatigue based on defect dipoles have been detailed [2–4,6]. It has also been proposed to use them to engineer high strain piezoelectric materials [7].

The existence of acceptor ion nearest neighbor oxygen-vacancy defect complexes could be established by electron paramagnetic resonance (EPR) of Fe^{3+} in cubic $SrTiO_3$, because of markedly different zero field splitting (ZFS) terms from the strong tetragonal crystal field resulting from the presence of the vacancy [8,9]. Electron magnetic resonance methods EPR and electron-nuclear double resonance (ENDOR) can provide direct information on the symmetry and distribution of the unpaired spin density, if couplings to magnetic neighbor nuclei can be resolved. Further, for $S = 1/2$ impurity ions there are no ZFS terms. In $PbTiO_3$, the presence of 22.1% ^{207}Pb nuclei with $I = 1/2$ can provide an excellent probe of the local environment surrounding the paramagnetic point defect.

Here we report on three Cu(II) impurity point defects in single crystal $PbTiO_3$ using EPR and pulsed ENDOR and establish local structure models for each based on the ^{207}Pb superhyperfine (SHF) couplings. It is found that Cu(II) substitutes for Ti; both the fully coordinated center with distant charge compensation and the defect dipole complex with an oxygen vacancy at an apical position are identified. The third center is found to be a $Cu(II)_{Ti}$-F^- defect with the fluorine ion substituting for an apical O^{2-} ion.

Measurements were performed using detwinned $PbTiO_3$ crystal grown at Argonne National Laboratory by a modified flux method [10]; no intentional dopants were introduced. EPR measurements were performed at 9.5 GHz

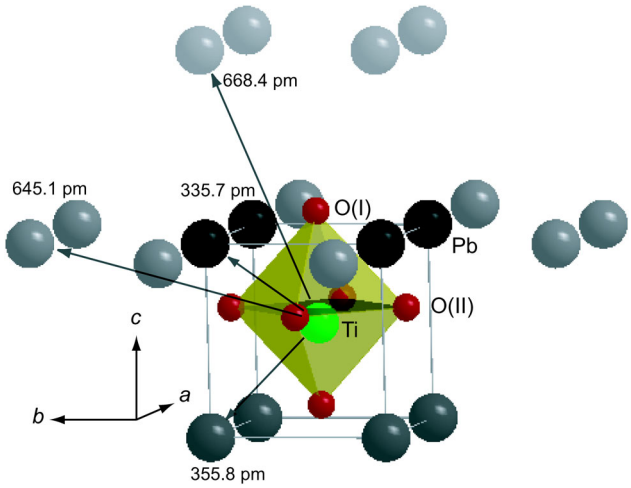

FIG. 1 (color online). 90 K $PbTiO_3$ crystal structure showing the unit cell and two further shells of equivalent Pb ions above the Ti site with associated Ti-Pb distances. The distances to similar shells below (not shown) are 655.8 (8 Pb) and 698.9 pm (4 Pb).

using a Bruker EMX spectrometer and an ER4122SHQ resonator and pulsed ENDOR measurements at 9.8 GHz using a Bruker E580 with an ER4118X-MD5-EN resonator. The Davis ENDOR pulse sequence, modified for enhanced polarization transfer (π-128 ns rf-π-10 μs π-32 ns rf-π-10 μs $\pi/2$–64 ns π-128 ns) [11], was used for ENDOR measurements. The EPR and ENDOR results were fitted to the spin Hamiltonian (SH) below using EASYSPIN [12]:

$$\hat{\mathbf{H}} = \mu_B \mathbf{B} \cdot g \cdot \mathbf{S} + \sum_i (\mathbf{I}_i \cdot \mathbf{A}_i \cdot \mathbf{S} - g_{n,i} \mu_n \mathbf{B} \cdot \mathbf{I}_i), \quad (1)$$

where μ_B and μ_n are the Bohr and nuclear magnetons, respectively, $g_{n,i}$ are the nuclear g factors, and the sum is taken over all relevant nuclei in the local environment. The first term describes the electronic Zeeman interaction with electronic spin S and is characterized by the g matrix, and the final term is the nuclear Zeeman interaction. The second term describes the hyperfine interactions; here the $i = 1$ term is the central hyperfine interaction with ^{63,65}Cu nuclei, and the $i > 1$ terms describe the SHF interactions with neighbor ^{207}Pb and ^{19}F nuclei. It is convenient to express the hyperfine tensors in terms of an isotropic hyperfine constant a and traceless tensor describing the anisotropic interaction $\mathbf{T}$, so $\mathbf{A} = a\mathbf{1} + \mathbf{T}$. The anisotropic tensor can be expressed in terms of two diagonal element parameters $b = T_{33}/2$ and $b' = (T_{11} - T_{22})/2$, describing the axial and orthorhombic contributions, respectively. For the SHF $\mathbf{A}$ tensors, a single off-diagonal asymmetry parameter $\Delta = A_{13} = -A_{31}$ can also be required [13].

The 20 K EPR spectrum for the Cu(II) centers is shown in Fig. 2(a), and the angular dependence of the line positions in the a-c plane in Fig. 2(b); the resulting SH parameters are listed in Table I. Center 1 is readily observed at room temperature, and center 2 is visible [14]. At lower temperatures, all three Cu(II) centers are resolved. Inversion recovery experiments measured the spin lattice relaxation times T_1 at 20 K for the three centers to be 6.2 ms, 0.66 ms, and 40 μs, respectively. The SH parameters are consistent with Cu(II) in an octahedral crystal field with a tetragonal distortion and $3d^9|x^2 - y^2\rangle$ as the ground state wave function. The g values can be related to the degree of splitting caused by the tetragonal distortion of the local environment; the g values decrease with increasing distortion [15]. Center 1 has the smallest g values.

In ferroelectric $PbTiO_3$, the oxygen octahedron is displaced "up" with respect to the Pb^{2+} and Ti^{4+} sublattices; see Fig. 1. The tetragonal distortion of the oxygen octahedron gives four equatorial oxygen ions (OIIs) equidistant from the Ti site, which at 90 K is displaced "below" the OII plane along the c axis by 32 pm toward the lower apical oxygen (OI) [16], giving a short strong bond, and a weak long bond to the upper OI. Substitution of an impurity ion with a charge different from Ti^{4+} will alter this bonding and is expected to result in a displacement off the Ti site along the c axis toward the center of the OII plane [4].

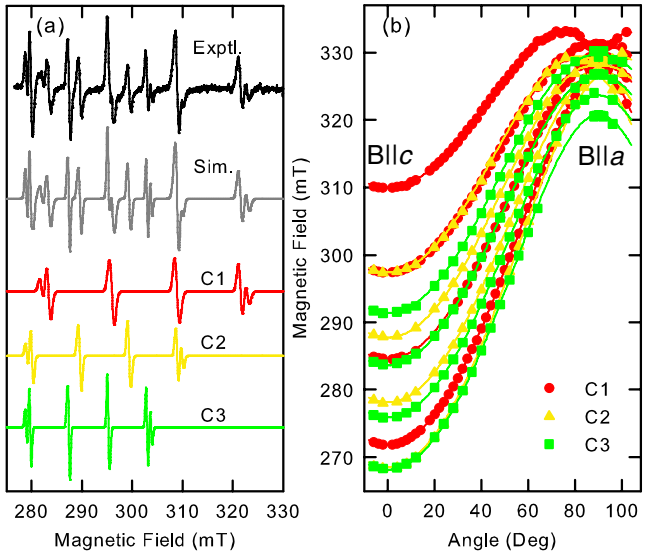

FIG. 2 (color online). (a) Experimental 20 K EPR spectrum at $B||c$ and best-fit simulation formed from summing three separate Cu centers simulations (C1, C2, and C3). (b) 20 K EPR ^{63}Cu line position a-c plane road map, center 1 (circle), center 2 (triangle), center 3 (square), and simulations (solid lines).

The ENDOR measurements were performed on each center in both the a-c plane (010) and the (110) plane, rotated 45° about the c axis, and additional off symmetry direction measurements were also made. Transitions due to three shells of equivalent Pb neighbor ions were identified for each center. In addition, center 2 showed a superhyperfine interaction with a single axial ^{19}F nucleus. The angular dependence of the ^{207}Pb lines for the first two shells of equivalent ions in the (010) plane, along with the ^{19}F lines for center 2, are shown in Fig. 3. The resulting SHF interaction tensor values are given in Table II. The direction of the largest principal SHF value, and of one other, lies in the plane containing the Pb ion, Cu(II), and the c axis. The angle β is defined from the line parallel to the c axis at the ion site to the direction of the largest principle value T_{33} and is taken as a counterclockwise rotation about the out-of-plane component (T_{22}). Several equivalent Euler angle sets, consistent with C_{4v} symmetry, exist.

All centers exhibit fourfold symmetry about the c axis, and the form of the ^{207}Pb ENDOR line angular dependence (Fig. 3) shows Cu(II) must substitute as an acceptor for

TABLE I. Electron paramagnetic resonance spin Hamiltonian values for Cu^{2+} centers in $PbTiO_3$ crystals. The ^{63}Cu hyperfine constants are given; only relative signs are determined.

T (K)	Center	$g_{\|\|}$	$g_\perp$	a/h (MHz)	b/h (MHz)
300	C1	2.340	2.057	138.0	129.0
	C2	2.404	2.075	120.3	90.3
20	C1	2.334	2.054	143.0	136.0
	C2	2.394	2.071	125.0	99.0
	C3	2.421	2.088	148.0	58.0

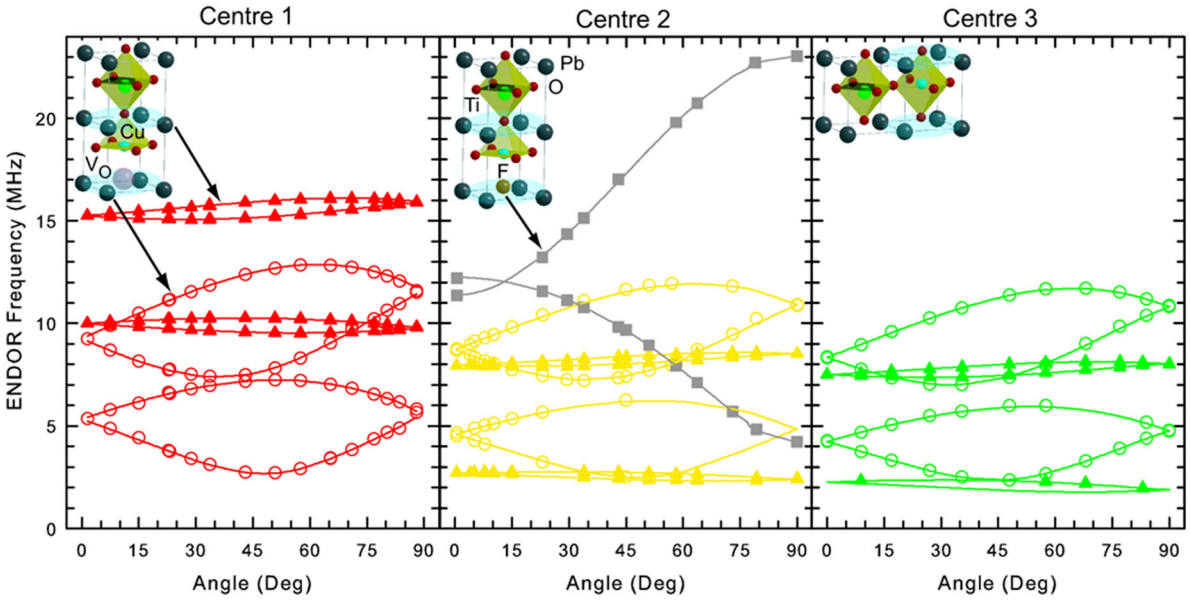

FIG. 3 (color online). ^{207}Pb ENDOR line position road maps in the a-c plane for centers 1 and 2 at 20 K and center 3 at 10 K. Additional lines due to ^{19}F are observed for center 2 (square). The schematic insets illustrate the defect model for the Cu impurity centers and the neighbor shells associated with the branches in the road maps; C1 has an apical oxygen, C2 has a F substituted at the oxygen-vacancy site, and C3 has a complete oxygen octahedron.

Ti^{4+} in each center. Shells I and II can be identified with the two nearest Pb ion shells above and below the $Cu(II)_{Ti}$ (Fig. 1). Moving from a high symmetry plane, the ENDOR lines split consistent with an interaction with 4 Pb ions in both shells. If the Cu(II) is displaced along the c axis to the expected position in the center of the OII plane, the distances to shells I and II given in Fig. 1 move further apart to 317.6 and 378.1 pm, respectively [16].

Table II shows that the ^{207}Pb shells I and II exhibit unusual behavior; the signs for the isotropic and anisotropic SHF constants are opposite for all three centers. Only relative signs are determined; however, large negative values for anisotropic constants have not been previously observed, while large negative isotropic constants can arise from the exchange polarization mechanism [17]. The large Pb s core is expected to be readily polarized. If the SHF interactions were due to overlap and covalency admixtures of the Pb^{2+} orbitals into a Cu(II)-O^{2-} complex alone, the a and b values would both be positive ($g_n > 0$) with $b \sim a/3$ [13]. We therefore assume the ^{207}Pb isotropic constants for shells I and II are negative.

The Cu $3d^9|x^2 - y^2\rangle$ orbital bonding to the equatorial oxygens will result in transfer of unpaired spin density to p orbitals perpendicular to the connection line from the OII to the neighbor Pb s core. Overlap admixtures of the neighbor s orbitals are then zero, but the exchange interaction causes a negative spin polarization of the Pb s core and hence a negative isotropic constant [17]. An admixture of Cu $3d^9|3z^2 - r^2\rangle$ character would evoke a similar exchange polarization of the Pb s core via OI.

From Table I it can be seen that centers 2 and 3 have quite similar g values; reflecting a similar crystal field, the Pb superhyperfine values are also similar (Table II). The ^{19}F ENDOR shows center 2 has a single F^- substituted for

TABLE II. Superhyperfine constants for Cu(II) centers in crystal $PbTiO_3$. Only relative signs could be determined; the values displayed assume that the Pb isotropic constants are negative.

Center	Shell	a/h (MHz)	b/h (MHz)	b'/h (MHz)	Δ/h (MHz)	β (deg)
C1	Pb_I	−25.4(1)	0.7(1)	−0.1(1)	3.0(1)	142(1)
	Pb_II	−14.9(1)	4.0(1)	−2.8(1)	2.5(1)	149(1)
	Pb_III	−3.0(1)	≤0.3	0	0	|40(3)|
C2	Pb_I	−10.8(1)	0.3(1)	−0.1(1)	1.1(1)	142(1)
	Pb_II	−13.8(1)	3.5(1)	−1.9(1)	2.1(1)	148(1)
	Pb_III	−2.3(1)	≤0.2(1)	0	0	|45(5)|
	F	−12.3(1)	6.6(1)	0.0(1)	0.0(1)	0(1)
C3	Pb_I	−9.8(1)	0.5(1)	−0.1(1)	0.5(1)	135(1)
	Pb_II	−13.5(1)	135(1)	135(1)	1.8(1)	149(1)
	Pb_III	−2.7(1)	≤0.2(1)	0	0	|45(5)|

one of the apical OI ions forming a Cu(II)-O_5F dipole defect. The negative a value of F^- is caused by the same exchange polarization mechanism but via the Cu $3d^9|x^2 - y^2\rangle$ and appropriate components of the OII p orbitals. However, the negative spin density, proportional to a/g_n [$g_n(^{207}\mathrm{Pb}) = 1.1748$, g_n (^{19}F) = 5.2577], is much lower than that on the Pb ions. We assign center 3 to Cu(II)-O_6, with a complete oxygen octahedron. The rather different Pb SHF values for the two Pb shells are expected from the relative positions of the oxygen octahedron and the Pb sublattice (Fig. 1) altering polarization and overlap effects. If Cu(II) moves upwards toward the OII plane, these differences may be accentuated.

Center 1 is assigned to the Cu(II)-oxygen vacancy, Cu(II)-O_5, dipole defect. The center has the smallest g values consistent with the largest tetragonal distortion. The positive Coulomb force on Cu(II) due to the oxygen vacancy is expected to move it up the c axis, possibly beyond the OII plane [4], causing admixture of the remaining OI oxygen so further enhancing exchange polarization of the ''upper'' shell Pb s cores consistent with the larger negative a value found for shell I. First principles calculations of impurity-ion oxygen-vacancy complexes in $PbTiO_3$ show the most stable position for the oxygen vacancy is at the ''lower'' short bond apical site [4,18]. We assign shell I to the upper set of 4 Pb ions for all centers. With this choice, insight on the direction of the SHF tensors can be gained using 180°-β for shell II; this is the angle obtained constraining T_{33} to point into the same unit cell for both shells. The relaxations of the shell II Pb ions results in similar SHF values for all three centers. A complete theory for the defects would require *ab initio* calculations that include correct treatment of relativistic Pb core states and the determination of SHF tensor values.

The anisotropic constants b can provide a direct measure of the distance to a given superhyperfine shell if dipole-dipole interaction contribution is dominant, and hence the isotropic component is negligible. Significant spin density transfer, by overlap, covalency, or polarization, invalidates such distance determinations and results in a deviation of the SHF tensor orientation away from the line joining the Pb neighbor with the Cu(II). Here even the distant third Pb shell has a dominant isotropic term (Table II). A recent hyperfine sublevel correlation spectroscopy (HYSCORE) study of Cu doped $PbTiO_3$ powders has reported ^{207}Pb SHF values for center 1 [19], for the shells corresponding to II and III shown here. There is good agreement for the isotropic constant values. However, the shell I interactions are too large to be observed by the standard HYSCORE. This led to the misassignment of shells, and the assumption that the dipole-dipole model could be used led to unrealistically small distances.

It is anticipated that the three Cu(II) defects identified here will also be present in PZT, but the reduction in tetragonality with increasing Zr content is expected to result in slight increases in g values and in changes to the overlap and covalency admixtures of the Pb^{2+} orbitals [20–22]. Improved dielectric and electromechanical properties have been reported for PZT ceramics codoped with a B-site acceptor (Mn or Mg) and fluorine [23]. Here we show F^- can form a stable nearest neighbor defect dipole complex with a divalent B-site acceptor, $Cu(II)_{Ti}$-O_5F, in $PbTiO_3$ substituting at an O^{2-} apical site, and provide evidence this occurs at the strong bond, lower, site.

In conclusion, three B-site substituted Cu^{2+} acceptor impurity defects have been observed by EPR and pulsed ENDOR, and their local structures identified. Two are defect dipoles, the Cu(II)-V_O and the Cu(II)-F^- complexes, and the third is Cu(II) with a complete oxygen octahedron.

This work was funded by the Research Councils UK Basic Technology Program (GR/S85726/01).

*d.j.keeble@dundee.ac.uk

[1] P. V. Lambeck and G. H. Jonker, Ferroelectrics **22**, 729 (1978).
[2] G. Arlt and H. Neumann, Ferroelectrics **87**, 109 (1988).
[3] G. E. Pike *et al.*, Appl. Phys. Lett. **66**, 484 (1995).
[4] S. Poykko and D. J. Chadi, Phys. Rev. Lett. **83**, 1231 (1999).
[5] M. Morozov, D. Damjanovic, and N. Setter, J. Eur. Ceram. Soc. **25**, 2483 (2005).
[6] D. C. Lupascu and U. Rabe, Phys. Rev. Lett. **89**, 187601 (2002).
[7] X. Ren, Nature Mater. **3**, 91 (2004).
[8] E. S. Kirkpatrick, K. A. Muller, and R. S. Rubins, Phys. Rev. **135**, A86 (1964).
[9] E. Siegel and K. A. Muller, Phys. Rev. B **19**, 109 (1979).
[10] Z. Li, M. Grimsditch, X. Xu, and S.-K. Chan, Ferroelectrics **141**, 313 (1993).
[11] C. Gemperle and A. Schweiger, Chem. Rev. **91**, 1481 (1991).
[12] S. Stoll and A. Schweiger, J. Magn. Reson. **178**, 42 (2006).
[13] J.-M. Spaeth and H. Overhof, *Point Defects in Semiconductors and Insulators* (Springer-Verlag, Berlin, 2003).
[14] D. J. Keeble, Z. Li, and M. Harmatz, J. Phys. Chem. Solids **57**, 1513 (1996).
[15] J. R. Pilbrow, *Transition Ion Electron Paramagnetic Resonance* (Clarendon Press, Oxford, 1990).
[16] A. M. Glazer and S. A. Mabud, Acta Crystallogr. Sect. B **34**, 1065 (1978).
[17] F. J. Adrian, A. N. Jette, and J. M. Spaeth, Phys. Rev. B **31**, 3923 (1985).
[18] H. Mestric *et al.*, Phys. Rev. B **71**, 134109 (2005).
[19] R. A. Eichel *et al.*, Phys. Rev. Lett. **100**, 095504 (2008).
[20] W. L. Warren *et al.*, J. Am. Ceram. Soc. **80**, 680 (1997).
[21] Z. Bryknar *et al.*, Appl. Phys. A **66**, 555 (1998).
[22] R. A. Eichel, H. Kungl, and M. J. Hoffmann, J. Appl. Phys. **95**, 8092 (2004).
[23] B. Guiffard, E. Boucher, L. Lebrun, and D. Guyomar, Mater. Sci. Eng. B **137**, 272 (2007).